Mon. Not. R. Astron. Soc. **000**, 000–000 (0000) Printed 1 February 2008 (MN LATEX style file v1.4)

Effects of Clumping on the Observed Properties of Dusty Galaxies

S. Bianchi[1⋆], A. Ferrara[2], J. I. Davies[1], P. B. Alton[1]
[1] *Department of Physics and Astronomy, Cardiff University, P.O. Box 913, Cardiff, CF2 3YB, UK*
[2] *Osservatorio Astrofisico di Arcetri, Largo E. Fermi 5, 50125 Firenze, Italy*

1 February 2008

ABSTRACT
We present Monte Carlo radiative transfer simulations for spiral galaxies modelled as a stellar disk and a two-phase clumpy dust distribution. We divide the volume occupied by the dust into a three-dimensional grid and assign each cell a clump or smooth medium status. Cell dimension, clump dust mass and spatial distribution are derived from the observed properties of Giant Molecular Clouds and molecular gas in the Galaxy. We produce models for several values of the optical depth and fraction of the interstellar medium residing in clumps. As a general result, clumpy models are less opaque than the corresponding homogeneous models. For the adopted parameters, the increase in the fraction of energy that escapes the disk is moderate, resulting in surface brightness profiles that are less than one magnitude brighter than those of the homogeneous models. The effects of clumping are larger for edge-on views of the disk. This is in contrast with previous preliminary results for clumping in the literature. We show how differences arise from the different parametrisation and clump distribution adopted. We also consider models in which a fraction of the stellar radiation is emitted within the clumps. In this case, galaxies are less transparent than in the case when only dust is clumped. The opacity can be even higher than in the homogeneous case, depending on the fraction of embedded stellar emission. We point out the implications of the results for the determination of the opacity and dust mass of spiral galaxies.

Key words: dust, extinction – ISM: cloud – galaxies: spiral– methods: numerical – radiative transfer – scattering

1 INTRODUCTION

An understanding of the effects of dust extinction in spiral galaxies is crucial, both for deriving the intrinsic properties of the galactic radiation field and interpreting observations of the distant universe in the background.

While in earlier studies the opacity of a galactic disk was often treated in a simplistic way, causing misinterpretations and mutually exclusive results (Disney, Davies & Phillipps 1989), a number of more realistic models has been developed in the last years; the radiative transfer have been modelled for appropriate galactic geometries, including multiple scattering, via analytical approximations (Byun, Freeman & Kylafis 1994; Silva et al. 1998) or Monte Carlo techniques (Bianchi, Ferrara & Giovanardi 1996, hereafter BFG; De Jong 1996; Wood 1997). Recently, the BFG code has been exploited to produce data for a conspicuous set of models (Ferrara et al. 1999, hereafter The Atlas).

The majority of the radiative transfer models for spiral galaxies deal with smooth distributions of dust and stars. Instead, the interstellar medium is observed to have a complex structure. It is difficult to solve the radiative transfer problem for a clumpy dust distribution. Therefore most models have been implemented for simple geometries. Analytical solutions for a clumpy plane parallel dust layer have been provided by Boissé (1990) for a two-phase medium and by Hobson & Scheuer (1993) for a generic N-phase medium, under the assumption of isotropic scattering. Witt & Gordon (1996) and Wolf, Fischer & Pfau (1998) performed Monte Carlo simulations for the radiative transfer through a spherical, two-phase dusty medium, illuminated by a central source. They divided the sphere in a cubic lattice, assigning each cell a low or high density status according to chosen values for the filling factor and density ratio of smooth/clump medium. Spherical clumps inside a spherical dust distribution have been studied by Városi & Dwek (1999), allowing radiation to come from a central point source, a uniform distribution of emitters, or a uniform distribution of external sources; analytical approximations are tested against Monte Carlo simulations.

⋆ Email address: Simone.Bianchi@astro.cf.ac.uk

We summarise here a few of the properties derived for clumpy distributions of dust. As a general rule, a clumpy medium has a higher transparency with respect to a homogeneous one with the same mass of dust. The effect of scattering is reduced, because light entering a dense clump has a low probability of escaping: from the point of view of the radiative transfer, a dense clump therefore behaves similarly to a dust grain with smaller albedo than the one characterising single grains in a smooth medium. For a clumpy distribution the amount of energy absorbed varies less with the wavelength of radiation than for a homogeneous distribution: this concurs, together with geometric effects (see The Atlas), in an apparent extinction, or more appropriately attenuation, curve flatter than the actual one.

However, the details of radiative transfer in a clumpy medium depend not only on the parameters used for the clumping itself, but also on the distribution of dust with respect to the stars. In this paper we present a study of the radiative transfer through a clumpy dust distribution for geometries typical of a spiral galaxy. Although the ISM may have a wide range of densities (Hartmann 1994; Heiles 1998), we adopt a simple two-phase scheme for the dust distribution: a smooth medium associated with the low-density diffuse atomic gas and clumps associated to high density Giant Molecular Clouds (GMCs). The distribution of clumps is derived from observations of the molecular gas in the Galaxy.

Only a few works include clumping in a radiative transfer model appropriate for galactic geometries. Kuchinski et al. (1998) use preliminary results from a Monte Carlo model (based on Witt & Gordon 1996 formalism) to derive opacities of edge-on galaxies from their colour gradients. Although a few aspects of the inclusion of clumping are presented in that paper, the authors defer a detailed discussion to a forthcoming paper. Clumping has been also included by Sauty, Gerin & Casoli (1998) in their model of the FIR and C^+ emission from the spiral galaxy NGC 6946; however, it is difficult to single-out the effect of clumping from the results shown.

Since star formation occurs in the dense phase of the interstellar medium, it is justified to assume that a fraction of the stellar emission occurs within clumps of dust. This may change the effects of clumping. In their model for a centrally illuminated dust distribution, Városi & Dwek (1997) find that the absorption efficiency may increase, rather than decrease, when clumps have a fractal distribution: being a fractal distribution a more connected set with respect to a uniform random distribution of spherical clumps, the fractal cloud can behave like a shield in front of the source. Embedded stars are included in the radiative transfer model of Sauty et al. (1998) and Silva et al. (1998). In this paper we will also consider the effects of a clumpy distribution for the radiation sources.

The paper is organised as follows. In § 2 we present a detailed description of the parameters used to describe the stellar emission and the clumpy dust distribution, referring to BFG and The Atlas for the general treatment of the radiative transfer; § 3 is dedicated to the effect of clumping for radiation coming from a smooth stellar distribution; § 4 shows the results when the possibility of sources embedded in dust clumps is taken into account. Finally, § 5 contains a summary and a discussion of the application of the results obtained in this work. Throughout the rest of this paper we will use the notation CM to refer to models including clumping and HM for homogeneous models.

2 THE MODEL

The results are obtained using an adapted version of the Monte Carlo code for the radiative transfer in dusty galaxies described in BFG. The original code has been simplified: a single Henyey-Greenstein scattering phase function (Henyey & Greenstein 1941; see also BFG) is used, with empirically derived values for the albedo ω and of the asymmetry parameter g. We use here the values $\omega = 0.6$ and $g = 0.6^{\dagger}$, appropriate for radiation in the V-band (Gordon, Calzetti & Witt 1997). The polarisation part of the radiative transfer code has been omitted. The same approach has been used for The Atlas.

In this paper we restrict ourselves to a single stellar spatial distribution, a three-dimensional disk with exponential behaviour in both horizontal and vertical directions. The horizontal and vertical scale lengths have been chosen to match the observed values for the old disk population of the Galaxy, $\alpha_\star = 3$ kpc (Kent, Dame & Fazio 1991; Fux & Martinet 1994) and $\beta_\star = 0.26$ kpc, respectively. Note that in BFG and in The Atlas we used $\alpha_\star = 4$ kpc (Bahcall & Soneira 1990): while in the previous models only the ratio between the scale lengths was relevant, for the model of this paper the absolute values must be specified, since the physical dimensions of the clumps are required (see later). The ratio between the horizontal and vertical scale lengths used in this paper is the same as in BFG and the Atlas.

Some specified fraction of the total dust mass is distributed in a smooth exponential disk, similar to the stellar one, with scale lengths $\alpha_d = \alpha_\star$ and $\beta_d = 0.4\beta_\star$ (BFG and Atlas), while the remaining mass is distributed in clumps.

The total mass of dust (smooth medium + clumps) is defined in terms of the optical depth of the model τ_V, i.e. the V-band face-on optical depth through the centre of the disk for a HM. For the exponential disk, the mass is easily computed using the formula

$$\begin{aligned} M_{\rm dust} &= \tau_V \, \alpha_d^2 \, \frac{8\pi}{3} \frac{a\delta}{Q_V} \, \left[1-(n+1)e^{-n}\right] \\ &= 6.8\times10^6 \, \tau_V \quad [{\rm M}_\odot] \, , \end{aligned}$$

where $a = 0.1\mu$m and $\delta = 3$g cm^{-3} are the grain radius and density, $Q_V = 1.5$ the extinction efficiency in the V-band (Hildebrand 1983) and $n = 4.6$ is the radial truncation of the disk (in scale length units; see later). In the following, when a CM is said to have been produced for a value of τ_V, it means that the CM has the same dust mass as a HM with a face-on V-band optical depth τ_V. Therefore, only in the case of a HM τ_V is a real optical depth, while for CMs is mainly an indicator of the mass of dust in the model, the effective opacity depending in a complex way on τ_V and the

† The values for ω and g are measured in Galactic reflection nebulae, by comparing the intensity of scattered light with radiative transfer models. Since a clumpy medium has a lower effective albedo, neglecting clumping in the model may bias the measure of ω towards lower values, especially for optically thick clouds and stronger forward scattering (Witt & Gordon 1996).

Table 1. Parameters of the clumpy distributions.

f_c	0.25		0.50		0.75		M_{dust}
τ_V	τ_V^s	N_c	τ_V^s	N_c	τ_V^s	N_c	$10^6 M_\odot$
0.1	0.075	255	0.05	511	0.025	784	0.7
0.5	0.375	1277	0.25	2554	0.125	3831	3.4
1.0	0.75	2554	0.5	5108	0.25	7662	6.8
2.0	1.5	5108	1.0	10215	0.5	15476	13.6
5.0	3.75	12769	2.5	25539	1.25	38308	34.0
10.0	7.5	25539	5.0	51077	2.5	76616	68.0

For each value of the fraction of gas in clumps f_c and of the optical depth τ_V, the optical depth of the smooth medium τ_V^s and the total number of clumps N_c are listed. The final column gives the total dust mass of the model.

other parameters for the clumpy dust distribution. Models have been produced for optical depths $\tau_V = 0.1, 0.5, 1, 2, 5, 10$.

Using a Galactic gas-to-dust ratio of 150 (Devereux & Young 1990; Sodroski et al. 1994), the gas mass can be derived from the dust mass. A fraction f_c of the total gas mass is then attributed to the molecular component. In this paper we explore three different values, $f_c = 0.25, 0.5, 0.75$. These values are representative of actual ratios observed in late type galaxies (from Scd to Sb, respectively; Young & Scoville 1991). All of the molecular gas (and the associated mass of dust) is supposed to be distributed in clumps. Our choice is appropriate, most of the molecular gas ($\approx 90\%$ in mass) in the Galaxy being in the form of GMCs (Combes 1991).

As for the clumpy structure, we use the same two-phase formalism as in Witt & Gordon (1996). The space occupied by dust is divided into cubic cells of the dimension of Galactic GMCs. Blitz (1991) quotes a typical diameter of 45 pc: a cubic cell of 36 pc will therefore have the same volume as a molecular cloud.

First, each cell is assigned a value corresponding to the local absorption coefficient (i.e. the inverse of the light mean free path through dust) for the smooth distribution of dust. If τ_V is the optical depth of the model, a fraction (1-f_c) of the dust mass is distributed in the smooth medium. Thus, the smooth medium opacity is defined by a face-on optical depth $\tau_V^s = \tau_V * (1. - f_c)$. The local absorption coefficient for the smooth medium is then computed from the assumed double-exponential distribution, using τ_V^s.

Second, we distribute the clumps. The position of each clump is derived from the distribution of molecular gas in the Galaxy, using the Monte Carlo method. We have used the CO observations of the first Galactic quadrant described by Clemens, Saunders & Scoville (1988). The radial density distribution has been derived from the plot of the mass of molecular hydrogen vs. galactocentric radius in their Fig. 11; we have adopted a gaussian vertical distribution, as parameterised in their Eqn. 3, with a FWHM that increases with galactocentric distance. Following the molecular gas, the distribution of clumps is more concentrated on the Galactic plane than the smooth dust. At any galactocentric distance, the probability of finding clumps for $|z| > 2.5\beta_d$ is nil. The distribution has been rescaled assuming 8.5 kpc as the Sun distance from the Galactic centre: the position of the Galactic molecular ring is thus between 1.5 and 3.5 radial scale lengths from the centre. Outside 13 kpc ($\approx 4.5\ \alpha_\star$) the molecular gas is not detected (see also Heyer et al. 1998). In the model, both the dust and the stellar disks are truncated at this distance from the centre.

Each clump has been given a typical GMC mass of 10^5 $M_\odot$ (Blitz 1993). The total number of clouds in the model is then directly derived from the mass of gas in clumps. Assuming that the dust has a uniform density inside each cloud, the absorption coefficient in the clump can be easily computed from the clump gas mass and dimensions, using the adopted dust properties and gas-to-dust ratio: each clump has an absorption coefficient in the V-band of 110 kpc^{-1}, corresponding to an optical depth $\tau_V \approx 4$. Since the effects of a clumpy structure are stronger when individual clumps are optically thick (Boissé 1990; Boissé & Thoraval 1996) our simulations provide an upper limit to the effects of clumping in a spiral galaxy.

For all the cells that have been assigned a clump status, the clump absorption coefficient is summed to the absorption coefficient of the smooth medium. The optical depth along any photon path is computed integrating the absorption coefficient array along the specified direction. Apart from this, the Monte Carlo code follows the same scheme as described in BFG. A list of the parameters defining the clumpy dust distribution is given in Table 1.

To reduce the computational time and the dimension of the array involved, we use only one octant of the galaxy and assign values in the other octant according to the model symmetries: the dust absorption coefficient is stored for 383x383x12 cells. Because of this, clumps are distributed randomly only in one octant. This does not affect the statistical properties of the model, as long as the number of clumps is large and the position of emission of photons is random. Nevertheless, we have tested the validity of this simplification comparing the results to a case with clumps distributed randomly all over the space, obtaining the same results. Finally, simulated images of 201x201 pixels are produced for several inclinations (BFG).

In the following sections, we present results and plots for a few representative cases of optical depth and inclination. The whole dataset of this paper is available at http://www.arcetri.astro.it/˜ sbianchi/clumping.html

3 RESULTS

As already described in the introduction, the main effect of clumping is that of an overall increase in the transparency

Table 2. Fraction of energy absorbed in each model.

	f_{emb}			0.00			0.15			0.50	
	f_c	0.00	0.25	0.50	0.75	0.25	0.50	0.75	0.25	0.50	0.75
τ_V											
0.1		0.02	0.01	0.01	0.01	0.09	0.08	0.08	0.25	0.25	0.25
0.5		0.07	0.06	0.05	0.04	0.13	0.12	0.11	0.29	0.28	0.28
1.0		0.12	0.11	0.09	0.07	0.17	0.16	0.15	0.32	0.31	0.30
2.0		0.19	0.18	0.15	0.12	0.24	0.22	0.19	0.38	0.36	0.35
5.0		0.32	0.31	0.28	0.23	0.37	0.34	0.30	0.49	0.47	0.44
10.0		0.44	0.43	0.39	0.34	0.48	0.45	0.40	0.59	0.57	0.54

For each value of τ_V, the first column gives the fraction for the HM ($f_c = 0$), then each group of three columns gives the values for CMs with a specific fraction of the total energy emitted within clumps (f_{emb}; $f_{emb} = 0$ refers to the case with a homogeneous stellar distribution) and for the three values of the fraction of gas in clumps f_c.

of the model. In Table 2 we show the fraction of the total energy that is absorbed in each model, as a function of τ_V (that defines the mass of dust) and f_c. Obviously, for the same value of the optical depth, more energy is absorbed in a HM (defined in the table by f_c=0.0). The results presented for the HM are the same as for the spiral galaxy disk in The Atlas. When the clumping is introduced, CMs with larger f_c are increasingly more transparent.

Within the same model, the effects of clumping depend also on the disk inclination. This is clearly shown in Fig. 1, where we have plotted the attenuation (i.e. the ratio between the observed flux and the intrinsic, unextinguished, total one) as a function of the optical depth, for the HMs and the CMs for three values of the inclination angles, i=20°, 66°, 90°. As seen before, CMs have the same attenuation as HMs with a smaller τ_V, for any inclination. The largest differences between the two cases are found in more face-on cases, and for high values of f_c. For instance, a face-on CM f_c=0.75 and optical depth $\tau_V = 10$ has the same attenuation as an HM with $\tau_V \approx 4$, while for an inclination of 20°, it corresponds to a HM with $\tau_V \approx 5$. For the same values of τ_V and f_c, the smooth medium has an optical depth τ_V^s=2.5.

The different behaviour of CMs with inclination can also be seen analysing the disk major axes profiles. In Fig. 2 and 3 we show the major axis profiles for two representative cases of low ($\tau_V = 1$) and high ($\tau_V = 10$) optical depth, for inclinations of i=20°, and 90°. In each left panel we plot with solid lines the profiles for CMs: the brighter profile always refers to the case with higher fraction of dust in clumps, $f_c = 0.75$, while the fainter is for $f_c = 0.25$. As a comparison, we have also plotted a series of profiles for HMs (dotted lines); the three brighter profiles have the same optical depth τ_V^s as the smooth medium in each of the CM, from $f_c = 0.75$ (upper profile) to $f_c = 0.25$. The faintest of the HM is characterised by the optical depth τ_V. The differences between each profile and the profile for the HM with optical depth τ_V are shown in the right panels, for the chosen inclinations.

As expected, a CM characterised by a value of τ_V and f_c has a major axis profile at an intermediate brightness between the HM of optical depth τ_V and the HM of optical depth τ_V^s, i.e. the homogeneous smooth component. The differences between HM and CM are not large, and always smaller than 1 mag. For optically thin cases, models are virtually indistinguishable at low inclinations (as in the $\tau_V = 1$ profiles of Fig. 2). For optically thick cases (e.g. the models in Fig. 3), the profiles for CM are closer to those for the smooth

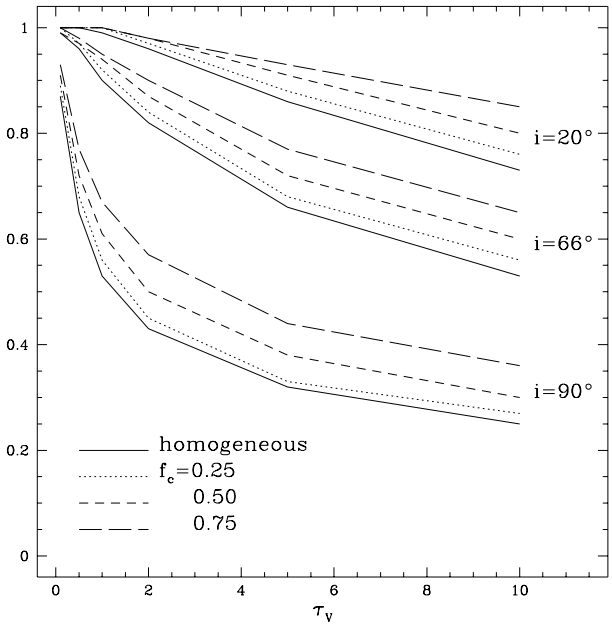

Figure 1. Attenuation as a function of the optical depth τ_V, for the HM and CMs with f_c=0.25, 0.50, 0.75. Data are plotted for three inclinations, i=20°, 66° and 90°.

medium only for $R < \alpha_\star$, where the number of clumps, and therefore their filling factor, is small. Between 1 and 3 $\alpha_\star$, where the molecular distribution peaks (the Galactic ring), the profile is closer to that for the HM with the same optical depth. On the contrary, profiles for edge-on cases are always brighter than the corresponding HM.

These results are in contrast with those presented by Kuchinski et al. (1998). They derived opacities of highly inclined galaxies, by comparing optical and near-infrared colour gradients with Monte Carlo radiative transfer simulations, including scattering and clumpy dust distribution. They found that the derived optical depths are insensitive to the dust having either homogeneous or clumpy distribution. This is explained by the significant number of clumps intersected by any line of sight through a nearly edge-on galaxy. On this basis they argue that clumping effects may be more important for lower inclinations, where some lines of sight

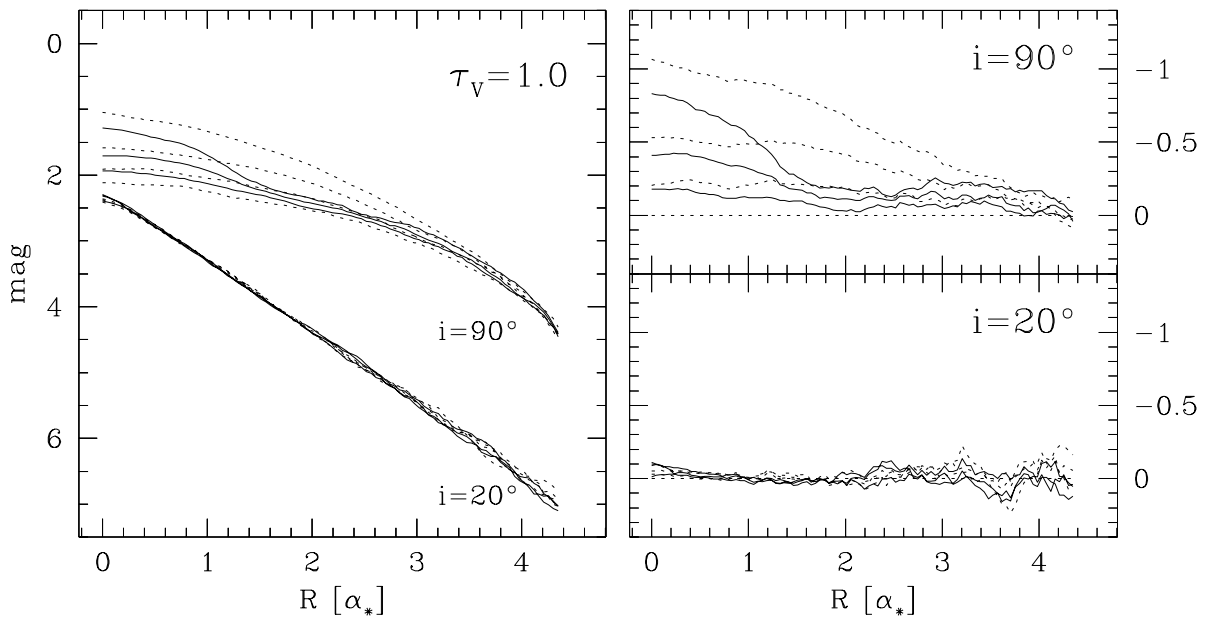

Figure 2. Major axis profiles (left panel) for models with τ_V= 1.0 and inclination i=20° (face-on), 90° (edge-on). Solid lines refer to CMs, for f_c= 0.25, 0.5, 0.75. The brighter profiles corresponds to the case with higher fraction of gas in clumps, f_c= 0.75, while the dimmer to the case with f_c= 0.25. HMs are presented for comparison (dotted lines). The brighter profile corresponds to a HM with the same optical depth as the homogeneous dust (τ_V^s) for the case f_c=0.75, followed by the analogous profiles for f_c= 0.5, 1.0. The dimmer profile refers to a HM with the optical depth τ_V. The right panel presents the difference in magnitude between each model and the HM with the optical depth τ_V. All curves have been smoothed with a box of 10 pixels.

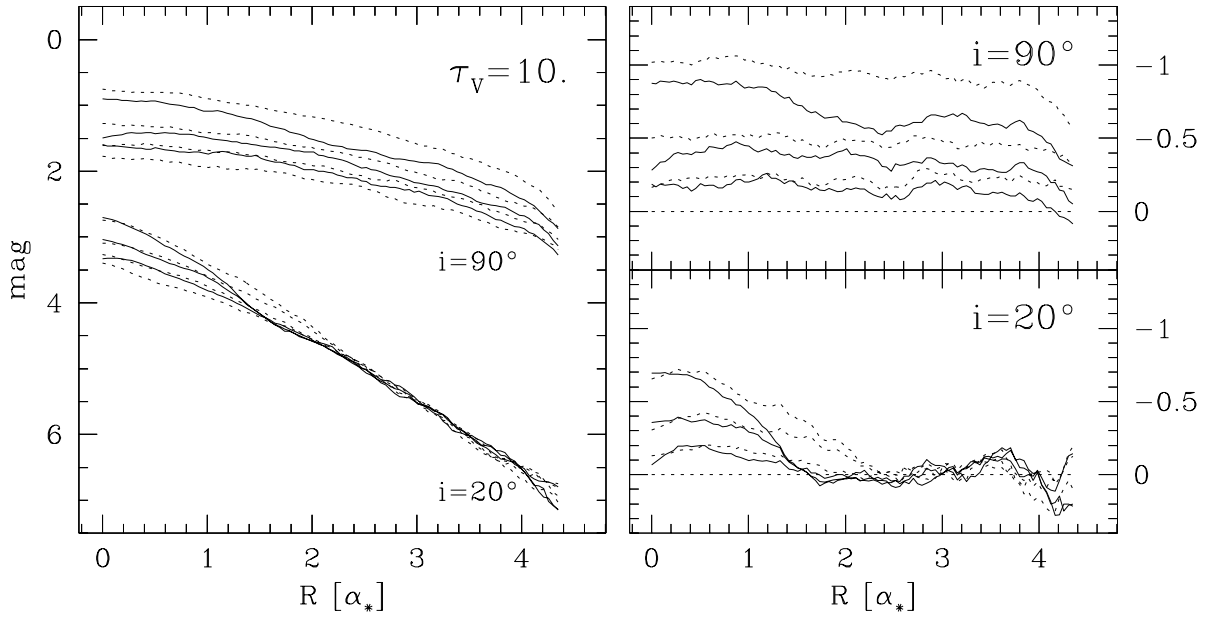

Figure 3. Same as Fig. 2, but for models with τ_V= 10.0. To avoid overlap, a constant value of 2 magnitudes has been subtracted from the surface brightness for the edge-on major axis profile presented in the left panel.

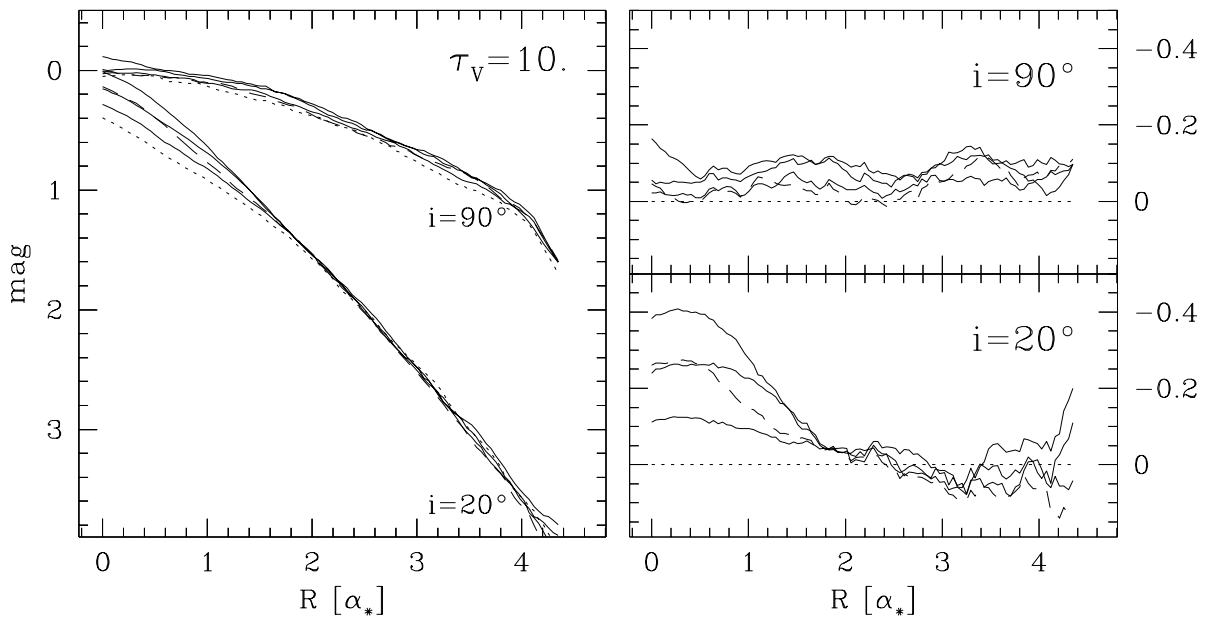

Figure 4. Major axis profiles (left panel) for CMs with constant filling factor all over the dust distribution and a ratio of 100 between densities in clumps and in the nearby smooth medium (See text for details). Models have τ_V=10 and i=20° and 90°. Solid lines refer to f_c= 0.25, 0.5, 1.0 (Brighter profile). With a dashed line the case f_c= 0.95 is plotted, while the dotted line refers to the HM with the same τ_V. To avoid overlaps, a constant value of 0.75 magnitudes has been subtracted from the surface brightness for the edge-on major axis profile. The right panel presents the difference in magnitude between each model and the HM with the optical depth τ_V. All curves have been smoothed with a box of 10 pixels.

pass across clumps, while others do not. However, the description of the clumpy structure of dust in Kuchinski et al. (1998) is different from the one adopted here. Following Witt & Gordon (1996), they assign a constant filling factor (ff=0.15) for the high density cells all over the galaxy, and assume a ratio of 100 between densities in clumps and in the nearby smooth medium. Since the smooth medium has an exponential distribution, clumps close to the galactic centre have a higher optical depth than those in the outer disk. Clumps in our simulations, instead, are distributed into a ring-like structure and have the same optical depth. We feel these assumptions are more realistic and are supported by the available observational data.

To clarify the reasons for the discrepancy, we have modified the code to deal with the Kuchinski et al. (1998) formalism. Clumps are now characterised by a constant filling factor all over the dust distribution and by a value for the local ratio of densities of the two dust phases. For these tests we have used the value 100 for the density ratio. The geometry of the galaxy and the cells dimensions have been kept as in §2. In Fig. 4 we show the major axis profiles in the case τ_V=10, for the two inclination i = 20° and 90°. The solid lines refer to CMs with the usual values f_c=0.25, 0.50, 0.75. In these models f_c can be directly converted into the filling factor ff using the formula

$$ff = \frac{f_c}{f_c + k(1 - f_c)},$$

where k = 100 is the density ratio. The f_c values of this paper thus correspond to quite low global filling factors, ff=0.003, 0.01, 0.03, respectively. The dashed line is for ff=0.15, as in Kuchinski et al. (1998). For the assumed density ratio, this value of the filling factor corresponds to $f_c \approx 0.95$, i.e. 95% of the total mass of dust in the model is distributed in clumps. Indeed, for this simulation setup, CMs have profiles closer to the HM when viewed at larger inclinations.

As for the profiles in Fig. 2 and Fig. 3, an increase of f_c in the range 0.25 - 0.75 produces an increase in the global transparency of the dust distribution, that is shown in Fig. 4 by the brighter profiles (especially in the face-on case) when a larger fraction of gas is distributed in clumps. The effects of clumping are instead reduced for f_c=0.95 (ff=0.15). This is consistent with the simulations of radiative transfer in a clumpy media presented by Városi & Dwek (1999). They have studied the case of a clumpy dust sphere under different radiation fields: a central source, a homogeneous distribution of isotropic emitters and a uniform external field. When all the other parameters defining the dust distribution are fixed, the fraction of absorbed photons as a function of the clumps filling factor shows a minimum, for any of the radiation fields. The exact value of ff for which the dust distribution has a maximum transparency depends on the details of the model. In our simulation, for the value of the clump/smooth medium density ratio adopted, clumping has the major effect in the reduction of the fraction of absorbed energy for $0.03 \leq ff < 0.15$ (or $0.75 \leq f_c < 0.95$). In the CM for f_c=0.95, 43% of the radiation is absorbed, almost the same quantity as for the f_c=0.25 case (and for the HM). As

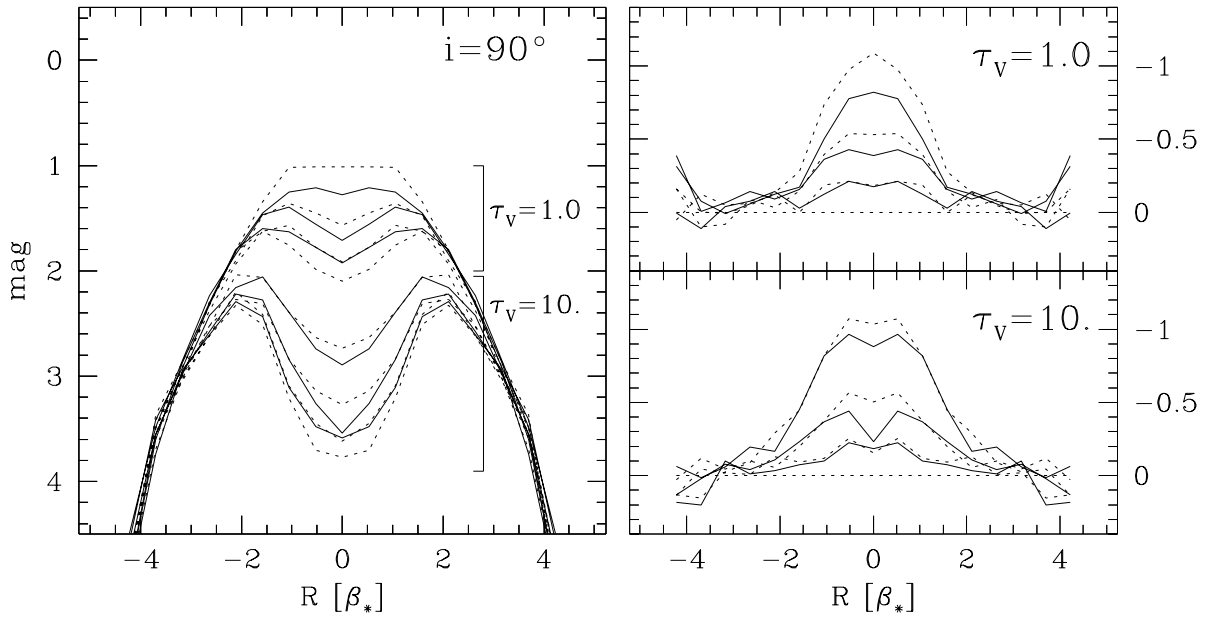

Figure 5. Edge-on (i = 90°) minor axis profiles (left panel) for models with f_c= 0.25, 0.5, 0.75 (solid lines). As in Fig. 2, brighter profiles corresponds to higher values of f_c. Dotted lines refers to HMs as described for Fig. 2. The right panel presents the difference in magnitude between each model and the HM with the optical depth τ_V.

already stated, the model for f_c=0.75 is more transparent, with 38% of the total radiation absorbed. With respect to the main models of this paper, the constant filling factor distributions are slightly more opaque, for the same value of f_c. In the τ_V=10 model with f_c=0.75 of Table 2, for instance, the fraction of absorbed energy is 34%.

The differences in behaviour between the main CM of this paper and the one with constant filling factor arise because of two reasons: (i) the different number of clumps for a given value of f_c and (ii) the different geometrical distribution. In the main CM clumps have all the same mass, and therefore the same density, for a given cell dimension. In the constant filling factor CM the density of a clump depends on the local density of the smooth medium (it is 100 times for the model analysed here). Because of the exponential distribution of the smooth medium, clumps at larger distance from the centre have smaller density (and mass) than those in the inner part of the galaxy. Consequently, when the fraction of ISM mass that is locked in clumps is fixed, the main CM will have a smaller number of clumps of higher mass than the one with a constant filling factor. For the case τ_V=10 with f_c=0.75 analysed before there are roughly 4 times more clumps in the latter than in the former. This smaller number of clumps is then distributed on preferential places in the main CM, more concentrated on the galactic plane and in the molecular ring. When seen face-on the large number of clumps in the ring position attenuates a lot of the radiation coming from the half of the galaxy below the plane, acting almost as a screen. Only outside the ring the filling factor of clumps is small, and in this regions the face-on profile is closer to that for a HM with the optical depth of the smooth medium. In the edge-on case, instead, it is the light emitted outside the ring, attenuated by the smooth dust distribution, that dominates the radiative transfer, thus resulting in a major axis profile of intermediate brightness between those of the HMs with τ_V and τ_V^s.

In Fig. 5 we plot the edge-on minor axis profiles for the main model with optical depths τ_V = 1 and 10. Geometrical and optical parameters of the dust distribution in spiral galaxies are mainly retrieved by fitting radiative transfer models to images of edge-on galaxies (Xilouris et al. 1997; Xilouris et al. 1998; Xilouris et al. 1999). At this inclination, in fact, we can have separate views of the radial and vertical dust distribution. Furthermore, dust extinction is increased as a result of the projection. The profiles of Fig. 5 show a behaviour analogous to the edge-on major axis profiles in Fig. 2 and 3, with a reduced extinction that results in shallower extinction lanes on the galactic plane. On the contrary, edge-on minor axis profiles for CMs with constant filling factor are virtually indistinguishable from the HM.

4 EMBEDDED SOURCES

So far clumping has been introduced only in the description of the dust distribution. Since we use a clumpy structure to simulate GMCs, it is logical to assume that part of the stellar emission comes directly from inside the clumps, the stars being formed in the higher density phases of the ISM. In this section we study the effects of clumping both for dust and stars.

Radiation from stars embedded in GMCs is simulated assuming that a fraction $f_{\rm emb}$ of the total energy emitted by stars comes from inside the clumps of dust. We have used

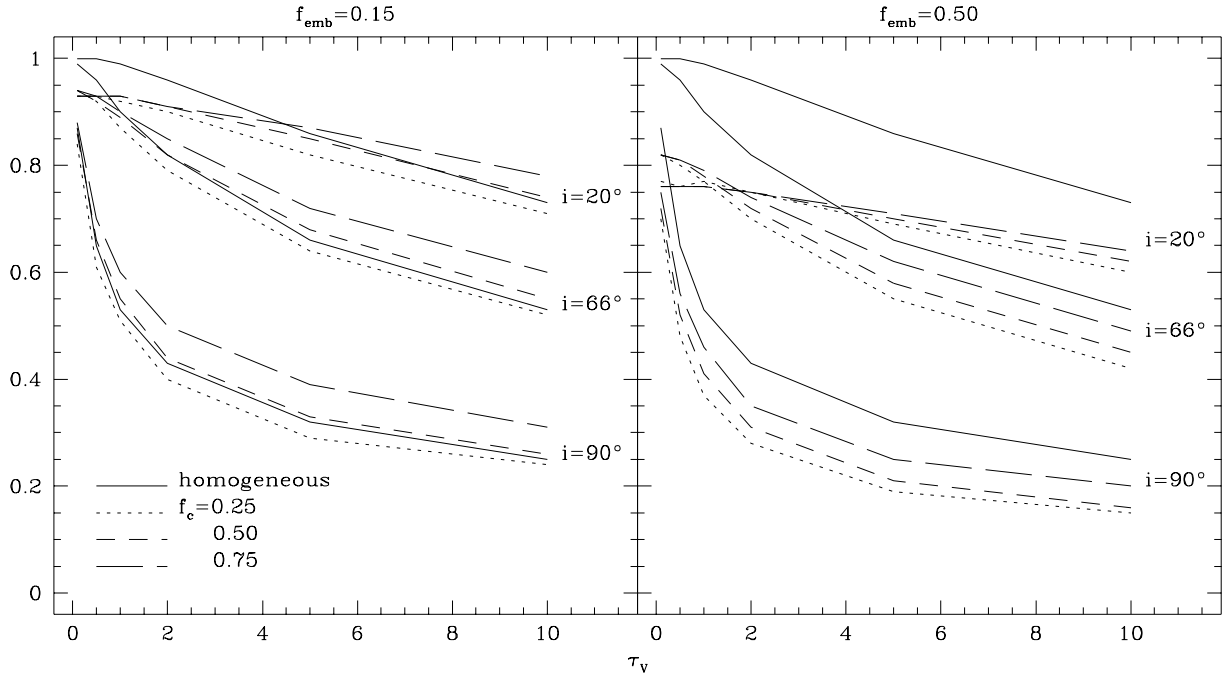

Figure 6. Same as Fig. 1, but for models with f_{emb}=0.15 and 0.50.

the values 0.15 and 0.50. The actual value of this parameter is difficult to be derived from observations, since it would require sensitive indicators of the (optically) obscured star formation rates. The above range is an educated guess that comes from the estimate of the average fraction of stellar lifetime spent inside dark clouds. Wood & Churchwell (1989) and Churchwell (1991), from their study of UCHII regions, concluded that O stars are embedded in their natal molecular clouds on average about 15% of the main sequence of an O6 star. However, this might be a lower limit and the fraction of total embedded star formation could be as high as 50% when the contribution from low mass stars is taken into account. Within the Monte Carlo code, a fraction $f_{\rm emb}$ of the photons is emitted inside the cells. The position of the emission inside the cell is randomly distributed within its boundaries. This allows more radiation to escape clumps, with respect to the case where the photons are emitted in the centre of the cell. Once the photon is emitted, the radiative transfer is carried out through the clumpy dust distribution as described in § 2.

The fraction of absorbed energy in CMs with embedding is shown in Table 2, for the two values of f_{emb}. In general, a larger fraction of energy is absorbed in these CMs with respect to the case when only dust has a clumpy distribution. The fraction of absorbed energy may be even larger than for a HM. When the degree of clumpiness increases (larger f_c) the effect of embedding is mitigated and more energy can escape. As an example, for $f_{\rm emb}$=0.15, optically thick CMs with $f_c \geq 0.5$ have an overall opacity similar or smaller than for the HM. The absorption in the case $f_{\rm emb}$=0.5 is larger and although it decreases with increasing f_c as for the previous case, the fraction of absorbed energy is always higher than in the HM. The large fraction of energy absorbed in the optically thin cases, especially for f_{emb}=0.5 might seem surprising. This is because in our formalism, for optically thin cases (small mass of dust), the embedded emission comes from relatively few opaque clumps. For a cubic cell of optical depth 4 through its side and with a homogeneous distribution of internal emitters, nearly 50% of the radiation is absorbed within the cell. For instance, in a model with τ_V=0.1 and f_{emb}=0.5, half of the radiation is emitted within clumps, and half of it is absorbed, thus resulting in a fraction of absorbed energy 0.25, as in Table 2.

The global increase in extinction can also be seen in the attenuation plots of Fig. 6. Models with clumping distributions for both stars and dust have a transparency lower than those with a clumpy dust distribution only, at any inclination. As already shown before, for $f_{emb} = 0.50$, all the CMs are more opaque than the corresponding HM with the same optical depth. For the more face-on inclinations, the behaviour of the attenuation is less dependent on τ_V with respect to the HM. This is because the projected optical depth of the smooth medium is lower, and the clumps dominate the emission (and absorption).

Face-on images, especially in the case for a higher fraction of embedded emission, clearly show a ring structure, due to the photons being emitted in clumps distributed accordingly to the ring-like distribution of molecular gas. When the models are seen edge-on, the ring is smoothed out by the projection and it is clearly visible only for optically thin cases and f_{emb}=0.50. In Fig. 7 we plot the major axis profiles for the edge-on cases with $\tau_V = 1$ and 10. For f_{emb}=0.15 and for optically thick models with f_{emb}=0.50, the major axis profiles are similar to those of HM with different effective opacities. It is interesting to note that the major axis profiles can be brighter than those of the HM with optical depth

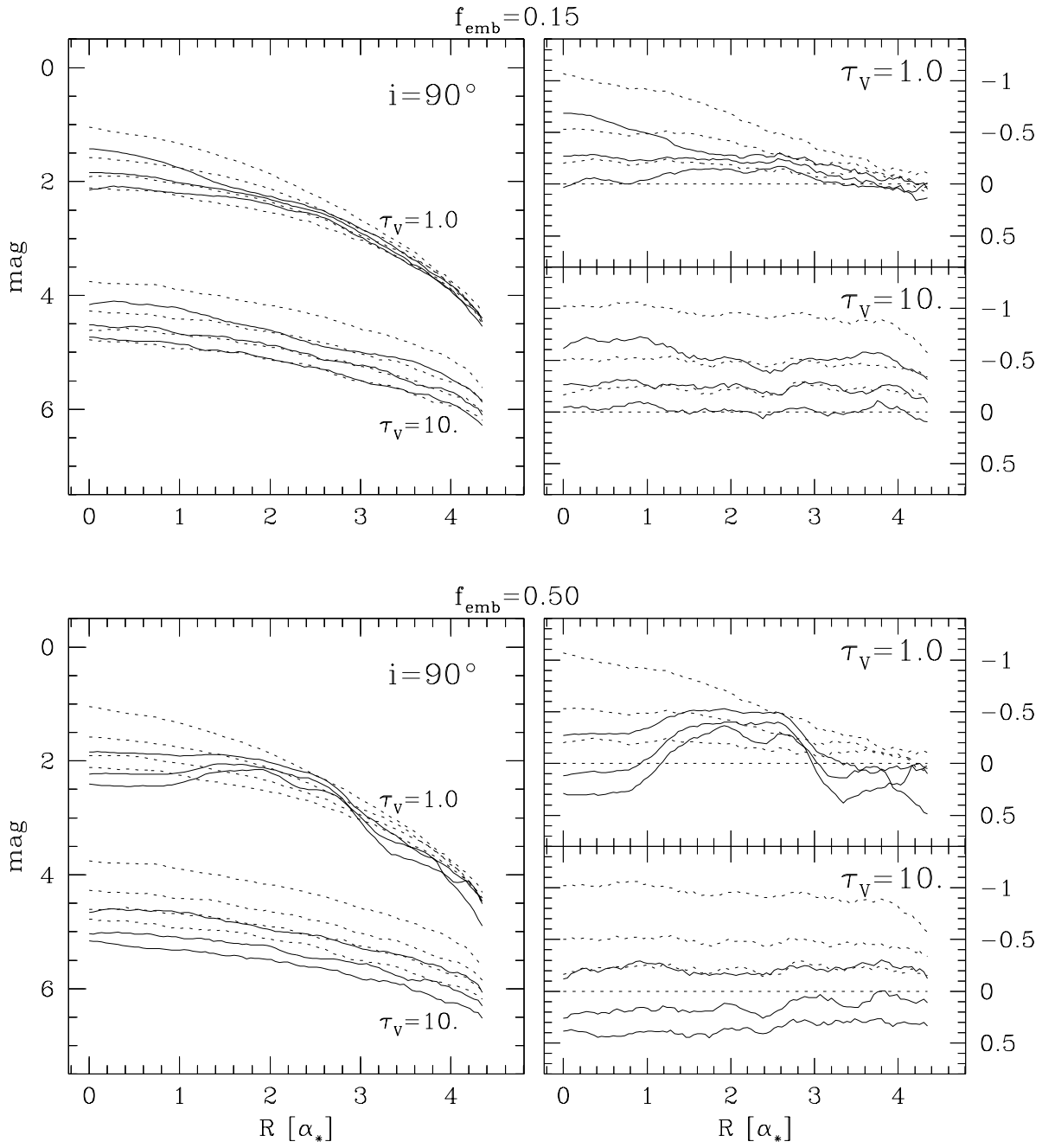

Figure 7. Edge-on major axis profiles (left panels) for models with embedded sources. Profiles are plotted for optical depths τ_V=1, 10 and for the three values of f_c (solid lines). As in Fig. 2, brighter profiles corresponds to higher values of f_c. Dotted lines refers to HM as described for Fig. 2. To avoid overlap, a constant value of 1 magnitude has been added to the surface brightness for the τ_V=10 profile. The right panel presents the difference in magnitude between each model and the HM with the optical depth τ_V. All curves have been smoothed with a box of 10 pixels.

τ_V, even when the global opacities are larger. For example, in an edge-on model with f_{emb}=0.50, f_c=0.75 and τ_V = 10 only 20% of the radiation escapes, while for the corresponding HM the fraction that escapes is 25%. The profile along the major axis is brighter, being very similar to that of the HM with τ_V=7.5. The brighter profile can be accounted for by the embedded emission, that is more concentrated in the plane than the smooth one. While the CM is generally dimmer than the HM, the major axis emission is higher: embedding concurs therefore with dust clumping in reducing the contrast of the dust edge-on absorption lane. This is clearly

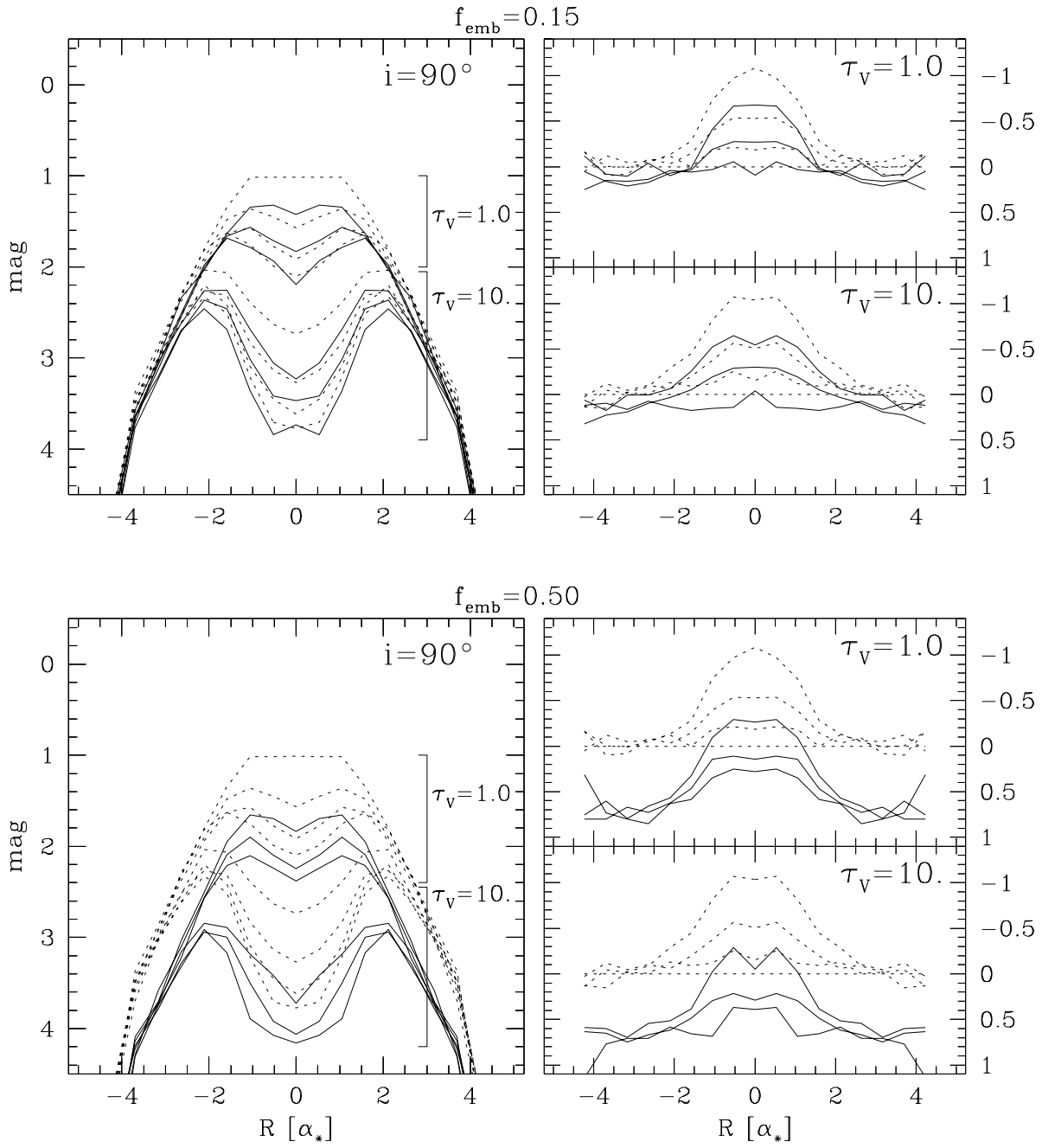

Figure 8. Edge-on minor axis profiles (left panels) for models with embedded sources. Profiles are plotted for optical depths τ_V=1, 10 and for the three values of f_c (solid lines). As in Fig. 2, brighter profiles corresponds to higher values of f_c. Dotted lines refers to HM as described for Fig. 2. The right panel presents the difference in magnitude between each model and the HM with the optical depth τ_V.

seen in the edge-on minor axis profiles in Fig. 8, especially for high optical depth and f_{emb}=0.50.

5 SUMMARY AND DISCUSSION

We have presented in this paper the results of Monte Carlo radiative transfer simulations through a two-phase clumpy dust distribution, for geometries typical of a spiral galaxy disk. The space occupied by the dust distribution has been divided into a three-dimensional grid and each cell has been assigned a clump or smooth medium status. The dimension of the cells and the dust mass of a clump have been derived from the properties of Galactic GMC. Clumps have been randomly distributed according to the ring-like distribution of molecular gas observed in our Galaxy. We have explored

several values for the optical depth τ_V (i.e. the optical depth of a homogeneous dust distribution with the same mass) and for the fraction of total gas residing in clumps.

The main conclusions are the following. As predicted by simple arguments and previous studies, a model with a clumpy dust distribution (CM) suffers a reduced extinction. For the parameters adopted in this paper, which emulate real dust distributions in spiral disks, the reduction of the fraction of absorbed energy is moderate, resulting in surface brightness profiles that are always less than one magnitude brighter than the corresponding homogeneous model (HM). The major differences between HMs and CMs are found for edge-on inclinations. This is in contrast to the results presented by Kuchinski et al. (1998). Using a model with spatially constant clump filling factor and with almost all (95%) of the galactic dust locked in clumps, they find that the smallest differences occur in edge-on cases. To ascertain the reasons for this discrepancy, we have reproduced their experiment and confirmed their results. We have concluded that the disagreement depends on the different parameters and distribution adopted for the clumps. This is unfortunate, however, as it indicates a strong dependence of the observed brightness profiles on the detailed internal and spatial distribution properties of clumps which makes the interpretation of the data very difficult.

Since star formation occurs in high density clouds, it is logical to assume that part of the stellar emission occurs within clumps. We have therefore produced models where a fraction of the photons is emitted in the high density cells. When this clumpy stellar distribution is considered, CMs are less transparent than for a clumpy dust distribution only. Depending on the fraction of gas in clumps and on the fraction of embedded stellar emission, galaxies can be even more opaque than predicted by HMs with the same mass.

One of the major concerns about clumping is that its neglect will produce a significant underestimate of the dust mass of a galaxy. Xilouris et al. (1999) analysed a sample of seven edge-on galaxies fitting the surface brightness with a radiative transfer model. They find a mean central face-on optical depth τ_V=0.5. Comparing the total dust mass of each galaxy with the mass of gas, they derive a gas-to-dust mass ratio of 360±60. The derived value is larger than the Galactic value by more than a factor of two (Sodroski et al. 1994), but closer than estimates based on FIR dust emission observed by IRAS (Devereux & Young 1990). From our results in Fig. 2 and Fig. 5, minor and major axis profiles for CMs with τ_V=1 and $0.50 < ff < 0.75$ are similar to those for a HM with $\tau_V = 0.5$ (In the $\tau_V = 1$ panels, a profile for a HM with $\tau_V = 0.5$ is shown between the two mentioned CMs with a dotted line). Therefore, a CM with $\tau_V = 1$ can have an edge-on appearance very similar to an HM with $\tau_V = 0.5$. The mass of dust in the CM would be twice the value derived for the HM and the gas-to-dust mass ratio would be reduced accordingly to 180, a value close to the canonical. Similar results can be obtained using the $\tau_V = 1$ profiles for models with embedded stellar emission. We caution here that Xilouris et al. (1999) find that dust disks have a larger radial scale lengths than the stellar while in the models of this paper both disks have the same radial scale lengths; this may affect the numerical details of the exercise carried out in this paragraph, but the qualitative result holds. On the contrary, a CM with a constant filling factor all over the galaxy would resemble, when seen edge-on, a HM with the same optical depth, and there would be no change in the mass estimate.

Acknowledgements. We wish to thank D. Galli for interesting discussion about the embedding of stars in molecular clouds and the referee, A. Witt, for useful comments that improved the presentation of the data in the paper.

REFERENCES

Bahcall J. N., Soneira R. M., 1980, ApJS, 44, 73
Bianchi S., Ferrara A., Giovanardi C., 1996, ApJ, 465, 127 (BFG)
Byun Y. I., Freeman K. C., Kylafis N. D., 1994, ApJ, 432, 114
Blitz L., 1991, in: The Physics of Star Formation and Early Stellar Evolution, eds. C. J. Lada, N. D. Kylafis, Kluwer, Dordrecht, p. 3
Blitz L., 1993, in: Protostar and Planets III, eds. E. H. Levy, J. I. Lumine, Univ. of Arizona Press, Tucson, p. 125
Boissé P., 1990, A&A, 228, 483.
Boissé P., Thoraval S., 1996, in: New Extragalactic Perspectives in the New South Africa, eds. D. L. Block , J. M. Greenberg, Kluwer, Dordrecht, p. 187
Churchwell, 1991, in: The Physics of Star Formation and Early Stellar Evolution, eds. C. J. Lada, N. D. Kylafis, Kluwer, Dordrecht, p. 221
Clemens D. P., Sanders D. B., Scoville N. Z., 1988, ApJ, 327, 129
Combes F., 1991, ARA&A, 29, 195
De Jong R. S., 1996, A&A, 313, 377
Devereux N. A., Young J. S., 1990, ApJ, 359, 42
Disney M., Davies J., Phillipps S., 1989, MNRAS, 239, 939
Ferrara A., Bianchi S., Cimatti A., Giovanardi C., 1999, ApJS, in press
Fux R., Martinet L., 1994, A&A, 287, L21
Gordon K. D., Calzetti D., Witt A. N., 1997, ApJ, 487, 625
Hartmann D., 1994, PhD Thesis, Sterrewacht Leiden
Heiles C., 1998, 1998, ApJ, 498, 689
Henyey L. G., Greenstein J. L., 1941, ApJ, 93, 70
Heyer M. H., Brunt C., Snell R. L., Howe J. E., Schloerb F. P., Carpenter J. M., 1998, ApJS, 115, 241
Hildebrand R. H., 1983, QJRAS, 24, 267
Hobson M. P., Scheuer P. A. G., 1993, MNRAS, 264, 145
Kent S. M., Dame T. M., Fazio G., 1991, ApJ, 378, 131
Kuchinski L. E., Terndrup D. M., Gordon K. D., Witt A. N., 1998, AJ, 115, 1438
Sauty S., Gerin M., Casoli F., 1998, A&A, 339, 19
Silva L., Granato G. L., Bressan A., Danese L., 1998, ApJ, 509, 103
Sodroski T. J. et al., 1994, ApJ, 428, 638
Városi F., Dwek E., 1997, in: The Ultraviolet Universe at Low and High Redshift, eds. W. H. Waller et al., AIP, New York, p. 370
Városi F., Dwek E., 1999, ApJ (1999), in press
Witt A. N., Gordon K. D., 1996, ApJ, 463, 681
Wolf S., Fischer O., Pfau W., 1998, A&A, 340, 103
Wood K., 1997, ApJ, 477, L25
Wood D. O. S., & Churchwell, E. 1989, ApJ, 340, 265
Xilouris E. M., Kylafis N. D., Papamastorakis J., Paleologou E. V., Haerendel G., 1997, A&A, 325, 135
Xilouris E. M., Alton P. B., Davies J. I., Kylafis N. D., Papamastorakis J., Trewhella M., 1998, A&A, 331, 894
Xilouris E. M., Byun Y. I., Kylafis N. D., Paleologou E. V., Papamastorakis J., 1999, A&A, 344, 868
Young J. S., Scoville N. Z., 1991, ARA&A, 581, 625